Modulation by K^+ channels of action potential-evoked intracellular Ca^{2+} concentration rises in rat cerebellar basket cell axons

Y. P. Tan and I. Llano

Arbeitsgruppe Zelluläre Neurobiologie, Max-Planck-Institut für biophysikalische Chemie, Am Fassberg, D-37070 Göttingen, Germany

(Received 12 April 1999; accepted after revision 14 June 1999)

1. Action potential-evoked $[Ca^{2+}]_i$ rises in basket cell axons of rat cerebellar slices were studied using two-photon laser scanning microscopy and whole-cell recording, to identify the K^+ channels controlling the shape of the axonal action potential.

2. Whole-cell recordings of Purkinje cell IPSCs were used to screen K^+ channel subtypes which could contribute to axonal repolarization. α-Dendrotoxin, 4-aminopyridine, charybdotoxin and tetraethylammonium chloride increased IPSC rate and/or amplitude, whereas iberiotoxin and apamin failed to affect the IPSCs.

3. The effects of those K^+ channel blockers that enhanced transmitter release on the $[Ca^{2+}]_i$ rises elicited in basket cell axons by action potentials fell into three groups: 4-aminopyridine strongly increased action potential-evoked $[Ca^{2+}]_i$; tetraethylammonium and charybdotoxin were ineffective alone but augmented the effects of 4-aminopyridine; α-dendrotoxin had no effect.

4. We conclude that cerebellar basket cells contain at least three pharmacologically distinct K^+ channels, which regulate transmitter release through different mechanisms. 4-Aminopyridine-sensitive, α-dendrotoxin-insensitive K^+ channels are mainly responsible for repolarization in basket cell presynaptic terminals. K^+ channels blocked by charybdotoxin and tetraethylammonium have a minor role in repolarization. α-Dendrotoxin-sensitive channels are not involved in shaping the axonal action potential waveform. The two last types of channels must therefore exert control of synaptic activity through a pathway unrelated to axonal action potential broadening.

Voltage-gated K^+ (Kv) channels are highly unevenly distributed in neurones. Evidence involving the use of specific antibodies directed against subtypes of Kv channels suggests a very precise targeting of specific molecular forms to the somato-dendritic and axonal compartments of brain neurones (Sheng *et al.* 1994). This subcellular distribution is particularly well established for the α-subunits of the Kv1 channels (e.g. Sheng *et al.* 1994; Wang *et al.* 1994; Table 1 in Veh *et al.* 1995 and references therein). In expression systems, Kv1 subunits form voltage-gated K^+ channels with a wide array of functional properties (Stühmer *et al.* 1989) that partially account for the enormous diversity of voltage-activated K^+ currents encountered in eukaryotic cells (reviewed by Coetzee *et al.* 1999).

These data raise the intriguing question of the role that specific K^+ channels could fulfill in axonal arborization. Perhaps the most basic role of K^+ channels is to control the resting potential. Because CNS neurones have long thin neurites, the value of the resting potential (or of the mean potential between action potentials) is not necessarily homogeneous throughout the entire cell. Thus, a major role of axonal K^+ channels is to set the local resting potential at strategic points of the axonal arborization. Through such regulation of resting membrane voltage at the site of action potential initiation, which is thought to be located in the axon (reviewed in Stuart *et al.* 1997), K^+ channels can alter the rate of neuronal firing. Control of the local resting potential at branching points could regulate the probability of action potential failure in the axonal arborization, as suggested by results at the CA3–CA1 synapse in hippocampal organotypic cultures (Debanne *et al.* 1997). A potential outcome of fine modulation of the axonal resting (or interspike) potential could be to allow some Ca^{2+} influx through voltage-gated Ca^{2+} channels. The resulting rise in $[Ca^{2+}]_i$ could have important consequences for the electrical properties of the axon, for example modification of propagation of the action potential (Lüscher *et al.* 1996), as well as on the probability of transmitter release, for instance following the activation of Ca^{2+}-dependent protein kinases (e.g. review by Xia & Storm, 1997). A second major

role of axonal K^+ channels, which is more widely appreciated, is to shape the repolarization of the axon potential once it is initiated, leading to a modulation of the resulting phasic presynaptic intracellular Ca^{2+} signal. A third role for axonal K^+ channels is to react to the previous electrical activity of the axon, either by cumulative inactivation of voltage-dependent K^+ channels (for example see Jackson *et al.* 1991), or by changing the resting K^+ conductance through activation of Ca^{2+}-dependent channels. Finally, certain axonal K^+ channels are modified following activation of ligand-gated presynaptic receptors such as $GABA_B$ receptors (reviewed in Wu & Saggau, 1997).

Establishing the functional role and pharmacology of K^+ channels in the central nervous system is an important goal not only for the basic understanding of signal processing, but also because these channels are promising targets for the development of specific neuroactive drugs. Progress concerning the pharmacological profile, spatial distribution and functional role of dendritic K^+ channels has been achieved through direct patch-clamp recordings in distal dendrites of hippocampal pyramidal cells (Hoffman *et al.* 1997). In the axon, this type of study is a challenging task because of the difficulties of accessing the axonal compartment and its synaptic terminals in brain preparations. Our current knowledge of the specific functions of axonal K^+ channels is very limited (see review by Röper & Pongs, 1996).

In the present work, we have measured the effects of various K^+ channel blockers on the action potential-evoked $[Ca^{2+}]_i$ rises recorded in single axonal varicosities of cerebellar basket cells with the help of two-photon laser excitation scanning microscopy. We selected cerebellar basket cells for several reasons. First, these neurones have a simple axonal arborization which is contained in a single plane (Ramón y Cajal, 1911) – a geometry which is very advantageous for presynaptic intracellular calcium imaging. Indeed, previous work from our laboratory has shown the feasibility of recording intracellular calcium signals at presynaptic varicosities in this preparation (Llano, Tan & Caputo, 1997). Second, the basket cell presynaptic terminal is a unique structure which is enriched with several subtypes of K^+ channel (see Discussion). Third, Southan & Robertson (1998*a*) have recently been able to obtain patch-clamp recordings directly from basket cell terminals. Their data on the effects of selected K^+ channel blockers can thus be directly compared with the results obtained in the present work.

METHODS

Sagittal cerebellar slices from rats aged 12–15 days were prepared according to procedures previously described (Llano *et al.* 1991). These procedures are in accordance with the guidelines for animal welfare followed by the Max-Planck Institute. Rats were decapitated after cervical dislocation. The slices were perfused (1·5 ml min^{-1}) with saline containing (mM): 125 NaCl, 2·5 KCl, 1·25 NaH_2PO_4, 26 $NaHCO_3$, 2 $CaCl_2$, 1 $MgCl_2$ and 10 glucose, equilibrated with a 95% O_2–5% CO_2 mixture (pH 7·3). All experiments were performed at room temperature.

Recordings of IPSCs from Purkinje cells

For tight-seal whole-cell recording of spontaneous inhibitory postsynaptic currents (IPSCs) from Purkinje cells, pipettes (tip resistance 2–2·5 MΩ) were filled with a solution containing (mM): 125 CsCl, 4·6 $MgCl_2$, 10 Hepes-Cs, 10 BAPTA-Cs, 1 $CaCl_2$, 0·4 Na_2-GTP, 4 Na_2-ATP (pH 7·3). Capacitance cancellation and series resistance compensation were done as described by Llano *et al.* (1991). Uncompensated series resistance values did not exceed 5–10 MΩ. To block ionotropic glutamate receptors, 10 μM 2,3-dihydroxy-6-nitro-7-sulphamoyl-benzene(*f*)quinoxaline (NBQX) and 100 μM D-aminophosphonovalerate (APV; Tocris, UK) were included in the extracellular solution. Bicuculline methochloride (1 μM; Tocris, UK) was also added in some experiments, to decrease IPSC amplitude thus avoiding the generation of action potentials which can be triggered by the largest IPSCs. Bicuculline was not used when the effects of apamin were tested, since it has recently been reported to inhibit apamin-sensitive K^+ channels (Seutin *et al.* 1997). Recordings started 2–4 min after breaking into the cell. Membrane potential was held at −60 mV and currents, filtered at 1·5 kHz, were sampled continuously at a rate of 250 μs per point with brief interruptions every 3 min to verify series resistance. To test the effects of K^+ channel blockers, 3–6 min of control synaptic activity was obtained, the drug to be tested was then added to the bath solution and the recording continued for an additional period of 6–10 min. Detection and analysis of IPSCs was done off-line and the mean amplitudes and mean frequencies of detected IPSCs were calculated for 20 s time bins. From these values, ratios of IPSCs amplitudes and frequencies in the antagonist over control were calculated and used to generate pooled data for statistical comparisons.

The K^+ channel antagonists α-dendrotoxin and apamin were purchased from Latoxan (France). Iberiotoxin was purchased from Alamone Labs (Israel). Other blockers (4-aminopyridine, charybdotoxin and tetraethylammonium chloride) were purchased from Sigma. Concentrated stocks of these antagonists were prepared in H_2O, except for 4-aminopyridine, which was dissolved in DMSO at a concentration of 500 mM.

Basket cell intracellular calcium monitoring

Basket cell identification and tight-seal whole-cell recordings were performed as detailed in Llano *et al.* (1997). In most experiments, pipettes (3·5–4·5 MΩ) were filled with a solution of the following composition (mM): 150 KCl, 4·6 $MgCl_2$, 10 Hepes-K, 0·4 Na_2-GTP, 4 Na_2-ATP (pH 7·3) and 200 μM of the K^+ salt of the Ca^{2+}-sensitive probe Oregon Green-1 (OG1; Molecular Probes, Eugene, OR, USA). For current-clamp recordings, the pipette solution contained (mM): 155 mM potassium gluconate, 6·6 KCl, 4·6 $MgCl_2$, 10 Hepes-K, 0·4 Na_2-GTP, 4 Na_2-ATP (pH 7·3) and 200 μM OG1. This solution was chosen to mirror the intracellular Cl^- concentration estimated in postnatal day (P)12–15 cerebellar interneurones (J. Chavas & A. Marty, unpublished results). Series resistance values in whole-cell recording ranged from 15 to 35 MΩ and were compensated for by 50–70%. In most of the experiments, 20 μM bicuculline, 10 μM NBQX and 100 μM APV were added to the extracellular solution. Most recordings were performed in the voltage-clamp mode in order to avoid the spontaneous firing of action potentials which occurs under current-clamp conditions.

We used a two-photon laser scan system optimized for scanning small subsections of the visual field at high repetition rates by driving galvanometric mirrors with frequency-enhanced, phase-compensated periodic signals (Tan *et al.* 1999). The excitation light was provided by a Tsunami mode-locked Ti:sapphire laser pumped by a Millennia diode pump cw visible laser (Spectra-Physics Lasers,

Mountain View, CA, USA). Laser wavelength was set to 820 nm. The laser beam was focused on a pair of galvanometric scan mirrors (G120 DT, General Scanning Inc., Watertown, MA, USA) mounted on a Zeiss Axioplan microscope (Zeiss, Germany). Power excitation at the specimen plane was limited to 6–8 mW by neutral density filters inserted in the optical path. Light was collected with a Zeiss × 63 water immersion lens (0·9 NA) and focused on an avalanche photodiode (SPCM-AQ-231; EG&G Optoelectronics, Vandreuil, Canada). The output of this detector was passed through a six-pole Bessel filter set at a corner frequency of 25 kHz, amplified and digitized at 10 μs sampling rate. Light signals were corrected for the non-linear input/output transfer function of the avalanche photodiode. The software for driving the galvanometric mirrors as well as for data collection and analysis was written in IGOR-Pro (Wavemetrics Inc, Lake Oswego, OR, USA). The 'Pulse Control' software modules provided by Dr Richard Bookman (University of Miami, USA) were used to control the A/D and D/A channels of an ITC-16 interface (Instrutech Corporation, USA). In the present work, we scanned areas of 26 μm × 10 μm or 13 μm × 9 μm with an effective pixel size of 0·25 μm × 0·25 μm (using the × 63 lens). The times per scan were 67·5 and 30·4 ms, respectively. For better time resolution, line-scan protocols were run at a speed of 0·76 ms line^{-1}.

This system is also equipped with a parallel excitation/recording pathway, consisting of a monochromatic light source and a CCD Camera (TILL Photonics, Germany) used to search for axonal structures and acquire light-transmitted images of the preparation. The experimental chamber and the patch-clamp micromanipulator were carried by an *x-y-z* table having three computer-driven DC motors (Physik Instrumente, Germany) which provided a convenient way to position the region of the cell to be scanned in the appropriate area of the visual field.

The standard protocol for studying intracellular calcium transients consisted of applying a sequence of 32 scans with no interval between consecutive scans. The series was started while the cell was held at −60 mV and a stimulus was applied at the end of the 4th or 8th scan. Fluorescence changes were analysed off-line by measuring the average fluorescence in small 'regions of interest' (ROIs; 25–36 pixels, corresponding to 1·56–2·25 μm^2) and converting it to the percentage change in fluorescence: $\Delta F/F_o = 100(F - F_r)/(F_r - B)$, where F is the measured fluorescence signal at any given time, F_r is the average fluorescence from the scans preceding the stimuli, and B is the mean value of the background fluorescence from four regions in the scanned field which do not contain any part of the dye-filled cell (see Fig. 1*Ab*). Because we kept excitation levels low to avoid cell damage, the basal fluorescence reported by OG1 in the axonal structures studied was usually less than 2 photons μs^{-1} (see example in Fig. 1*Ca*). However, the signals were unambiguously distinguished from the much lower background in the surrounding areas. The inherent confocality of the two-photon excitation eliminated any problems related to image blurring by out-of-focus fluorescence, facilitating signal analysis.

To assess the dynamic range of OG1, *in vitro* calibrations were performed in the two-photon set-up, using 820 nm as the excitation wavelength. K^+-based solutions with $[Ca^{2+}]_i$ values ranging from 17 nM to 40 μM were prepared from the calcium calibration buffer kit No. 2 (Molecular Probes, USA) and 25 μM OG1 was added to each sample. The estimated K_d was 90 nM. Assuming a basal $[Ca^{2+}]_i$ of 40 nM, the calibration curves predict that OG1 saturation will be reached for $\Delta F/F_o$ of ~380 %.

Statistical analysis

All statistical values in the text are given as means ± S.E.M. When assessing the effects of K^+ channel blockers, means and S.D. of the logarithm of the individual values were calculated for different experimental groups and compared using Student's t test; P values < 0·05 were considered significant and are denoted in Fig. 8 with an asterisk on top of the corresponding histogram. The pooled data in Fig. 8 correspond to the geometric means ± S.E.M.

RESULTS

Action potential-evoked axonal $[Ca^{2+}]_i$ rises in cerebellar basket cells

Figure 1 shows fluorescence images acquired in a basket cell terminal using the fast scanning two-photon microscope, at rest (*Aa*) and at the peak of the $[Ca^{2+}]_i$ rise induced by a train of short depolarizing pulses (*Ab*). The position of the scanned region, identified by the rectangle in the light-transmitted image shown in Fig. 1*B*, includes part of a Purkinje cell soma. At the zone of contact with the Purkinje cell, the axon ramified and extended two distinct thick presynaptic terminals along the soma. The soma of the recorded basket cell was voltage clamped at a holding potential of −60 mV. The stimuli used throughout this work to elicit intracellular calcium transients consisted of 3 ms pulses to 0 mV either applied in isolation or in short trains, with 20 ms interpulse intervals. This frequency was chosen because it is near the firing rate of basket cells *in vivo* (Eccles *et al.* 1966). Several lines of evidence demonstrate that short voltage pulses applied to cerebellar interneurones under whole-cell recording produce a propagated axonal action potential. First, in paired recordings of interneurones and Purkinje cells, evoked IPSCs which are elicited by action potentials fired spontaneously from an unperturbed interneurone (when the latter is recorded in cell attached) have similar amplitude distribution and time course to those evoked by short depolarizations applied to the interneurone in whole-cell recording (Vincent & Marty, 1996). Second, under our experimental conditions, the intracellular calcium signals recorded at axonal sites located at distances of 40–300 μm from the cell soma had indistinguishable time courses and amplitudes for pulse durations ranging from 0·5 to 5 ms (data not shown). Third, numerical simulations of the voltage distribution along the axons of cerebellar interneurones indicate that the voltage-clamp protocol used in the present work elicits propagated action potentials in the axon (Pouzat & Marty, 1999). Furthermore, we find that the intracellular calcium transients elicited by short depolarizing pulses under voltage-clamp conditions have amplitudes and temporal courses similar to those evoked by action potentials in current-clamp conditions (see Fig. 5).

In the experiment shown in Fig. 1, a train of eight pulses was delivered. The resulting changes in fluorescence were non-homogeneously distributed within the synaptic terminal, as evident in the $\Delta F/F_o$ image shown in Fig. 1*Ac*. The temporal course of the action potential-evoked signals is plotted in Fig. 1*Ca* and *b* for three defined regions of interest (ROIs; see Methods) where large $\Delta F/F_o$ transients were recorded. The signals reached their peak within three scans (202·5 ms; time per scan, 67·5 ms), corresponding to

the end of the stimulus train, and decayed to 50 % of their peak value within 500 ms. In accord with our previous study of depolarization-evoked $[Ca^{2+}]_i$ rises in axons of Cs^+-loaded basket cells (Llano *et al.* 1997), trains of action potentials elicited $[Ca^{2+}]_i$ rises not only in synaptic terminals onto Purkinje cell somata but also in regions of the axon corresponding to axonal branch points and varicosity-like axonal enlargements. An example of such a $[Ca^{2+}]_i$ rise in an axonal branch point is shown in Fig. 2, where *Aa* displays the area of the axon being scanned and *Ab* plots $\Delta F/F_o$ as a function of time for the ROI drawn on *Aa* over the branch point. The different traces in *Ab* correspond to the responses to one, two and four action potentials. For the train of four pulses, the signals rise within three scans (91·2 ms; time per scan, 30·4 ms), again reaching their peak at the end of the stimulus train. For one pulse the peak is reached within one scan and line scans at 0·76 ms per line were performed to resolve the rise time. The line scan through the centre of this branch point is shown in Fig. 2*Ba*; the corresponding plot of $\Delta F/F_o$ *versus* time is shown in Fig. 2*Bb*. Peak $\Delta F/F_o$ is reached 6 ms after the stimulus.

We analysed in a similar fashion synaptic terminals on Purkinje cell somata, branching points, and axonal varicosities from 20 basket cells. The peak amplitude and rise time for the intracellular calcium signals evoked by trains of four action potentials, determined from scans of the type shown in Figs 1 and 2, were $114 \pm 6{\cdot}9$ % and $129 \pm 4{\cdot}3$ ms; they decayed within 204 ± 14 ms to half their peak value (52 ROIs from 20 cells). The decay time will reflect the combined action of endogenous buffers, of the Ca^{2+} indicator and of the cell Ca^{2+} clearance systems.

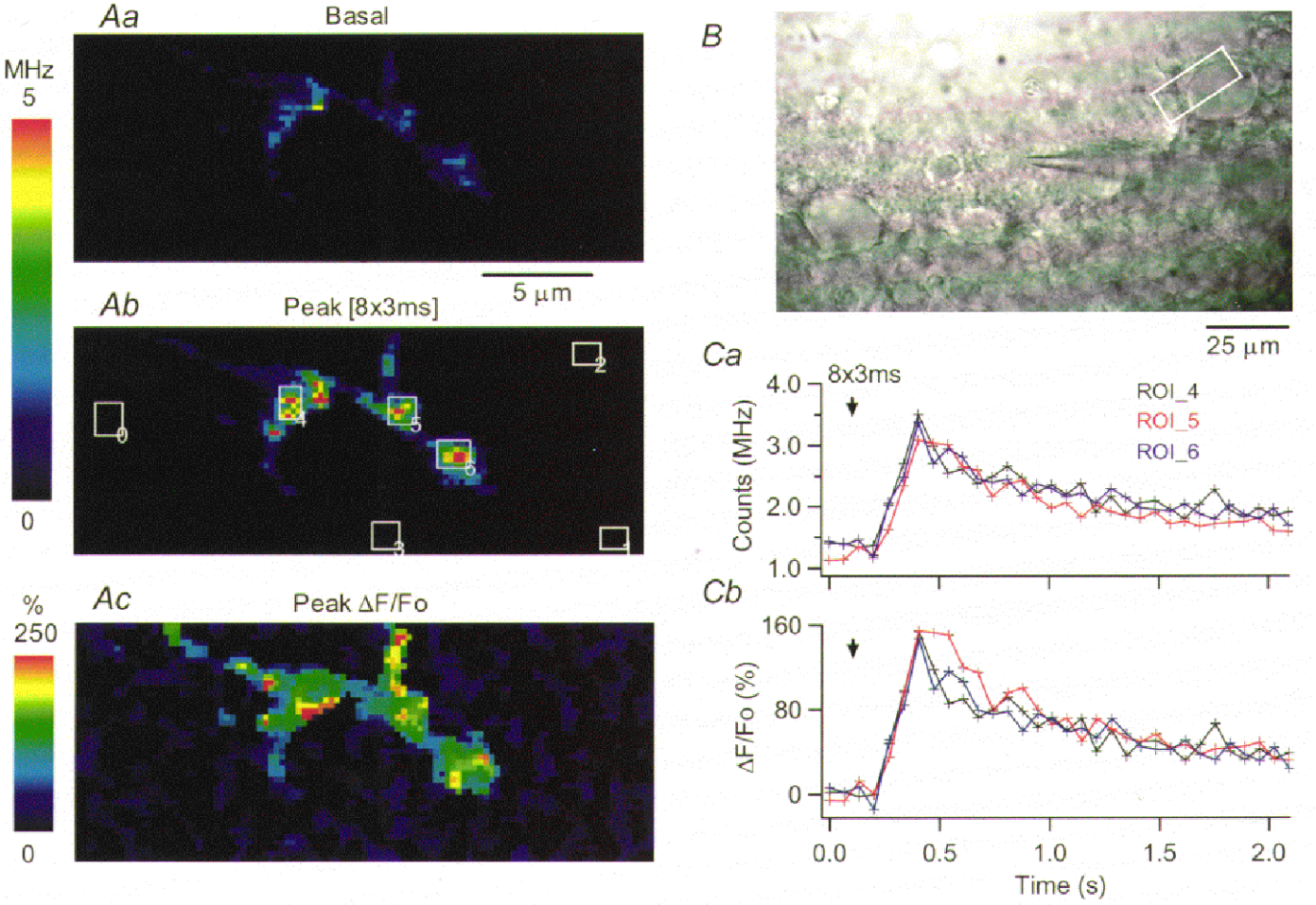

Figure 1. $[Ca^{2+}]_i$ rises evoked in a basket cell presynaptic terminal by a train of action potentials

A, pseudocolour images constructed from the OG1 fluorescence measured during scans of 26 μm × 10 μm and 67·5 ms dwell time, at rest (*Aa*) and at the peak of the response to eight action potentials (*Ab*). *Ac* shows the $\Delta F/F_o$ image at the peak of the $[Ca^{2+}]_i$ rise. *B*, light-transmitted image of the slice. The white rectangle delimits the area scanned, which contains part of a Purkinje cell soma. The basket cell soma is ~40 μm to the left, in contact with the recording pipette. *Ca*, plot of the average photon counts as a function of time, for three ROIs on this presynaptic terminal. ROI positions are given by the rectangles drawn in *Ab*. *Cb* plots the corresponding temporal evolution of the relative changes in fluorescence for the three ROIs. The arrows in *Ca* and *Cb* mark the onset of the train of action potentials. Here and in subsequent figures, to emphasize stimulus-driven fluorescence changes, pseudocolour images are displayed at a scale which saturates for some regions. However, the original data in which analysis was performed were not saturated.

The influence of the exogenous buffer on the measured time of decay depends on the cell Ca^{2+}-binding ratio (reviewed by Neher, 1995) which is unknown for basket cells. However, basket cell axons have high levels of the calcium binding protein parvalbumin (Kosaka *et al.* 1993), a property they share with cerebellar Purkinje cells. The Ca^{2+}-binding ratio in Purkinje cells (Fierro & Llano, 1996) is orders of magnitude higher than that reported for glutamatergic CNS neurones where this parameter has been determined (reviewed by Neher, 1995). It is thus reasonable to expect that basket cells will be endowed with a high buffering power. Thus, the effects of a high affinity Ca^{2+} indicator on the amplitude and time course of intracellular calcium transients should be smaller than those reported for glutamatergic axons which have a low Ca^{2+}-binding ratio (Regehr & Atluri, 1995; Helmchen *et al.* 1997; Sinha *et al.* 1997). Consistent with these arguments, the time to half-decay derived from this work is of the same order of magnitude as that reported for trains of eight action potentials in axonal varicosities imaged with the low affinity indicator Calcium Green 5N (~350 ms; Llano *et al.* 1997).

The intracellular calcium transients elicited by single action potentials were often below our detection level. In cells in which they could be properly analysed, their amplitude was $52 \pm 5{\cdot}3$ % (27 ROIs from 12 cells); the rise time determined from line scan protocols in eight of these ROIs was $7 \pm 0{\cdot}5$ ms. This rise time is significantly slower than the expected duration of the action potential driven Ca^{2+} influx. Measurements with a low affinity indicator will be required to determine if the kinetics of OG1 distort the rise time, as observed in other preparations (Regehr & Atluri, 1995; DiGregorio & Vergara, 1997).

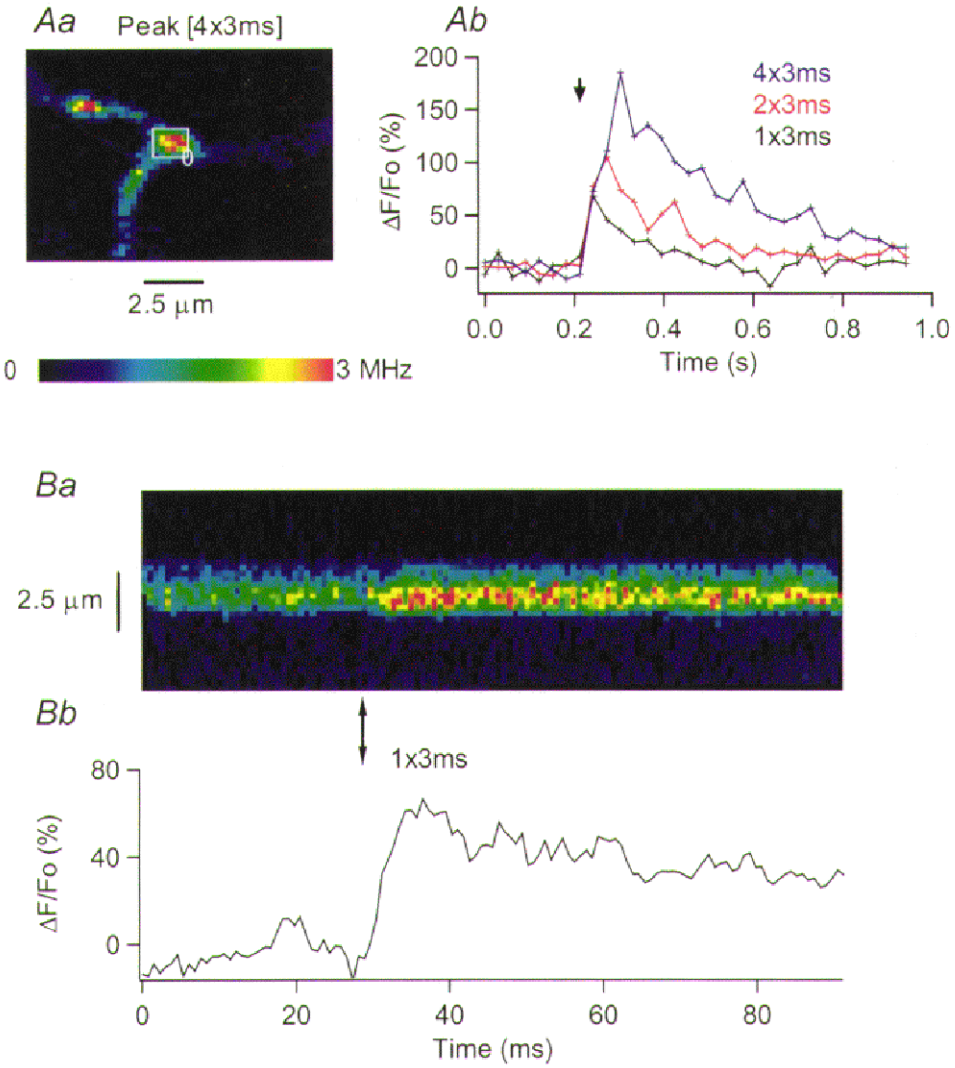

Figure 2. Action potential-evoked $[Ca^{2+}]_i$ rises in an axonal branch point

Aa, pseudocolour image from a scan of 13 μm × 9 μm and 30·4 ms dwell time, obtained at the peak of the response to a train of four action potentials. The rectangle indicates the area analysed in *Ab*, where the time course of the $\Delta F/F_o$ signals elicited by one, two and four action potentials is plotted as a function of time. *Ba*, pseudocolour image of a line scan through the centre of the branch point. The vertical arrow below the image marks the time when a single action potential was delivered. *Bb* plots the time course of the $\Delta F/F_o$ values. The pseudocolour calibration bar in *A* applies also to the line scan image shown in *B*.

We found that, provided that the excitation power was kept below 6–8 mW at the specimen plane, the electrical parameters of the cell, such as the amplitude of the holding current and of the Na^+ and K^+ voltage-gated currents, as well as the size and time course of intracellular calcium transients, were quite stable during recording periods of up to 2 h. This allowed us to pursue experiments in which long control and test periods were required, as described in the next section.

Effects of K^+ channel blockers on action potential-evoked axonal $[Ca^{2+}]_i$ rises

We used action potential-evoked $[Ca^{2+}]_i$ rises to gain insight into the nature of the K^+ channels responsible for shaping the action potential waveform in basket cell axons. Given the enormous diversity of K^+ channels present in eukaryotic cells (reviewed by Coetzee *et al.* 1999), we first screened a variety of pharmacological agents known to block K^+ channels, including α-dendrotoxin (αDTX), 4-aminopyridine (4-AP), charybdotoxin (CTX), iberiotoxin (Ibtx), apamin and tetraethylammonium (TEA) chloride for their effect on the spontaneous release of GABA, by recording IPSCs from Purkinje cells. The effects of some of these agents are shown in Fig. 3. The traces in Fig. 3*A–C* present samples of continuous recordings from three cells obtained in control external saline (upper traces) and after addition of a K^+ channel antagonist (lower traces). Figure 3*D* illustrates the analysis of two different experiments, by plotting mean IPSC amplitude and frequency throughout the recordings. The upper panel contains an experiment in which αDTX increased both parameters, whereas the lower panel shows an experiment in which apamin failed to affect the synaptic

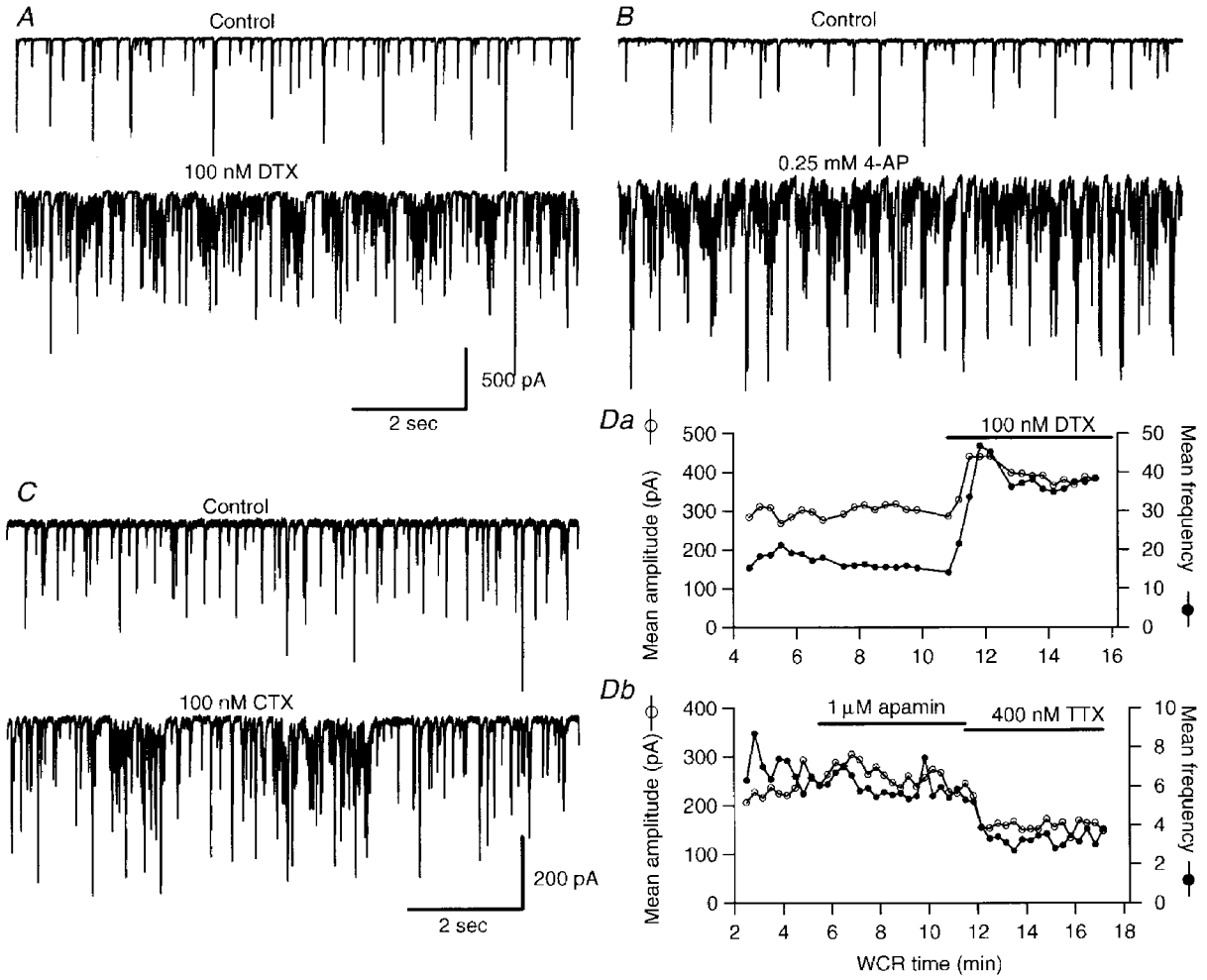

Figure 3. Effects of K^+ channel antagonists on Purkinje cell IPSCs

A–C, representative traces of spontaneous IPSCs recorded from three Purkinje cells before (upper panels) and after (lower panels) the addition of 100 nM αDTX (*A*), 0·25 mM 4-AP (*B*) and 100 nM CTX (*C*). The calibration bars in *A* apply also to the experiment shown in *B*. *D*, plots of the mean IPSCc amplitude (○) and mean frequency (●) calculated for 20 s time bins, as a function of whole-cell recording (WCR) time. *Da*, shows an experiment in which αDTX was applied, while in the experiment shown in *Db* apamin was tested. NBQX (10 μM), APV (100 μM) and bicuculline (1 μM) were present throughout the recordings shown in *A–C* as well as in the experiment shown in *Da*. In the experiment shown in *Db* 10 μM NBQX and 100 μM APV were present, but no bicuculline was added to avoid possible effect of this drug on apamin-sensitive K^+ channels (Seutin *et al.* 1997).

activity. In this case, TTX was added towards the end of the experiment, to ascertain that the synaptic activity included action potential driven neurotransmitter release. In this series of experiments, with the exception of apamin and Ibtx, all of the compounds tested significantly increased the release of GABA from cerebellar interneurones, as evidenced by their effect on the rate and amplitude of Purkinje cells IPSCs (see pooled data in Fig. 8*B* below). The channels affected by these agents are thus all candidates for contributing to the repolarization of the action potential in presynaptic structures. We note that our data differ from a recent study comparing IPSCs in wild-type and Kv1.1 mutant mice which reports that, in wild-type mice, αDTX and 4-AP increased the frequency but not the amplitude of IPSCs (Zhang *et al.* 1999).

We first focused on the effects of αDTX. This toxin is a selective blocker of the Kv1.1 and Kv1.2 channels (Table 1 in Mathie *et al.* 1998) both of which are enriched in basket cell terminals (McNamara *et al.* 1993, 1996; Sheng *et al.* 1994; Wang *et al.* 1993, 1994). Expression of Kv1.1 and Kv1.2 α-subunits *in vitro* results in αDTX-sensitive voltage-dependent K^+ currents with gating properties resembling those of the classical delayed rectifier currents (Stühmer *et al.* 1989; reviewed by Mathie *et al.* 1998). Furthermore, direct recordings from basket cell terminals in mouse cerebellar slices have recently shown that their voltage-activated K^+ currents are reduced by αDTX (Southan & Robertson, 1998*a*). However, we found that the action potential-evoked $[Ca^{2+}]_i$ rises in basket cell terminals were not affected by this toxin. This result is illustrated in Fig. 4, which analyses the intracellular calcium signals evoked in a basket cell terminal by trains of four action potentials. The axonal region scanned is shown for the control condition in Fig. 4*Aa* and *b*. It co-localized, as in Fig. 1, with a Purkinje

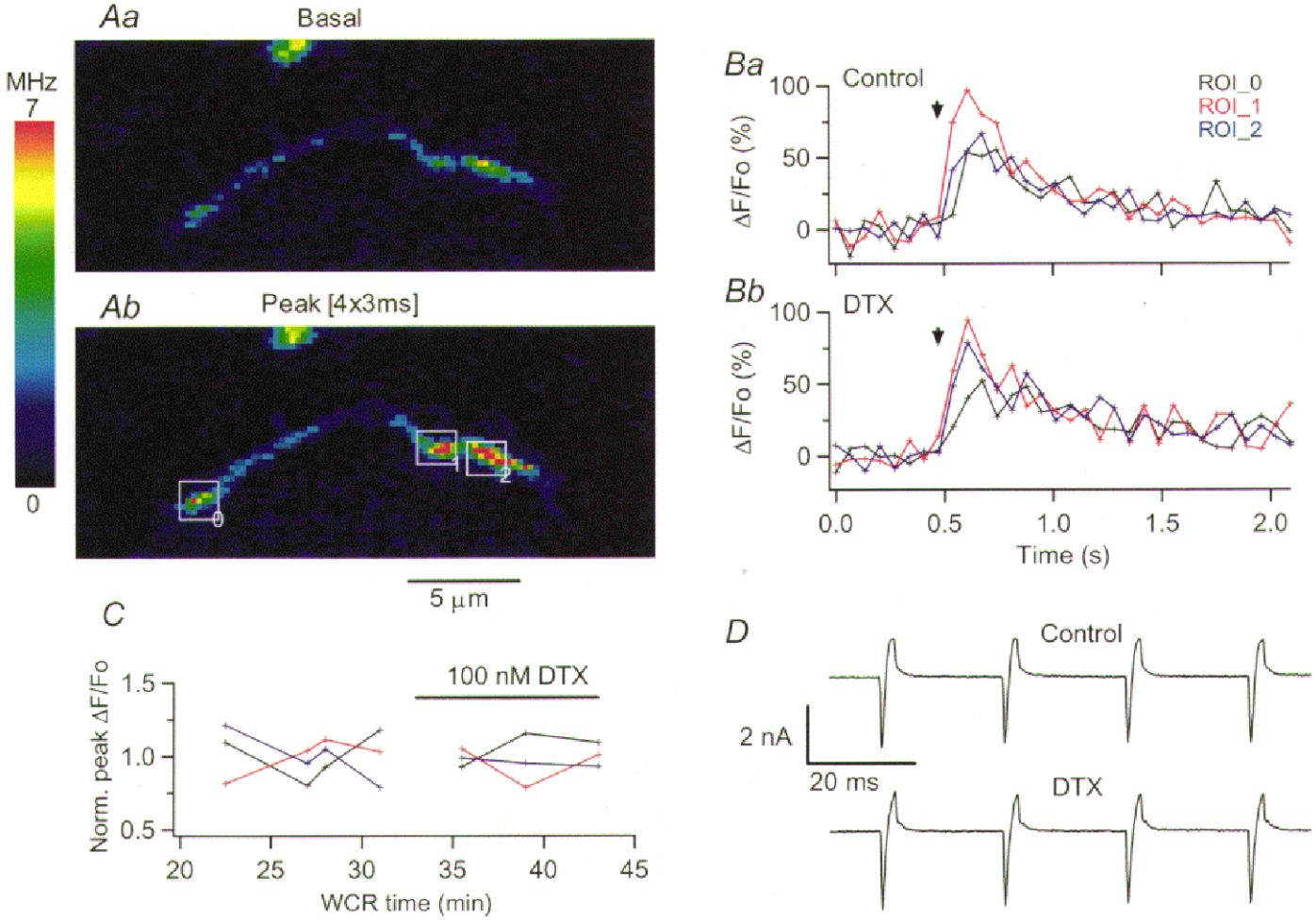

Figure 4. Action potential-evoked $[Ca^{2+}]_i$ rises in basket cell terminals are not affected by αDTX

A, pseudocolour images obtained in control external saline at rest (*a*) and at the peak of the response to four action potentials (*b*). The positions of the three ROIs analysed in *B* and *C* are given by the rectangles drawn in *b*; this terminal co-localized with a Purkinje cell soma. *B* displays the time course of the $\Delta F/F_o$ signals evoked by the four action potentials in the three ROIs, in control saline (*a*) and in the presence of 100 nM αDTX (*b*). In *C*, the peak $\Delta F/F_o$ signals for each ROI were normalized to the average of the four responses obtained in control condition, and plotted as a function of whole-cell recording time. *D* shows the ionic currents recorded at the soma during the depolarizing trains in control (upper trace) and in the presence of αDTX (lower trace).

cell soma. The time course of the $[Ca^{2+}]_i$ rises in three ROIs of this basket terminal is displayed in Fig. 4*Ba* (in control saline) and *b* (8 min after addition of 100 nM αDTX). There is no change in the signals. Figure 4*C* plots the peak $\Delta F/F_o$ for the three ROIs, normalized to the average value in control saline, as a function of whole-cell recording time. It can clearly be seen that αDTX failed to affect the peak amplitude of the $[Ca^{2+}]_i$ rises. Similar results were obtained in seven cells, where terminals on Purkinje cell somata, branching points or axonal varicosities were analysed (see review in Fig. 8*A*). Furthermore, and in accord with the results of Southan & Robertson (1998*a*), we found that this toxin does not affect the currents recorded from the basket cell soma (Fig. 4*D*).

To test whether these results were influenced by the stimulation protocol, experiments were performed under current-clamp conditions in cells loaded with an intracellular solution designed to resemble the physiological Cl^- gradient (see Methods). Figure 5 presents data from one of these experiments. The axonal intracellular calcium transients elicited by short depolarizing trains applied under voltage-clamp conditions from a holding potential of −70 mV had a time course and an amplitude similar to those evoked by trains of action potentials under current calmp conditions (Fig. 5*D*; the corresponding current and voltage traces are shown in Fig. 5*B* and *C*). As shown in Fig. 5*D* and *E*, αDTX failed to affect the intracellular calcium transients evoked by action potentials under

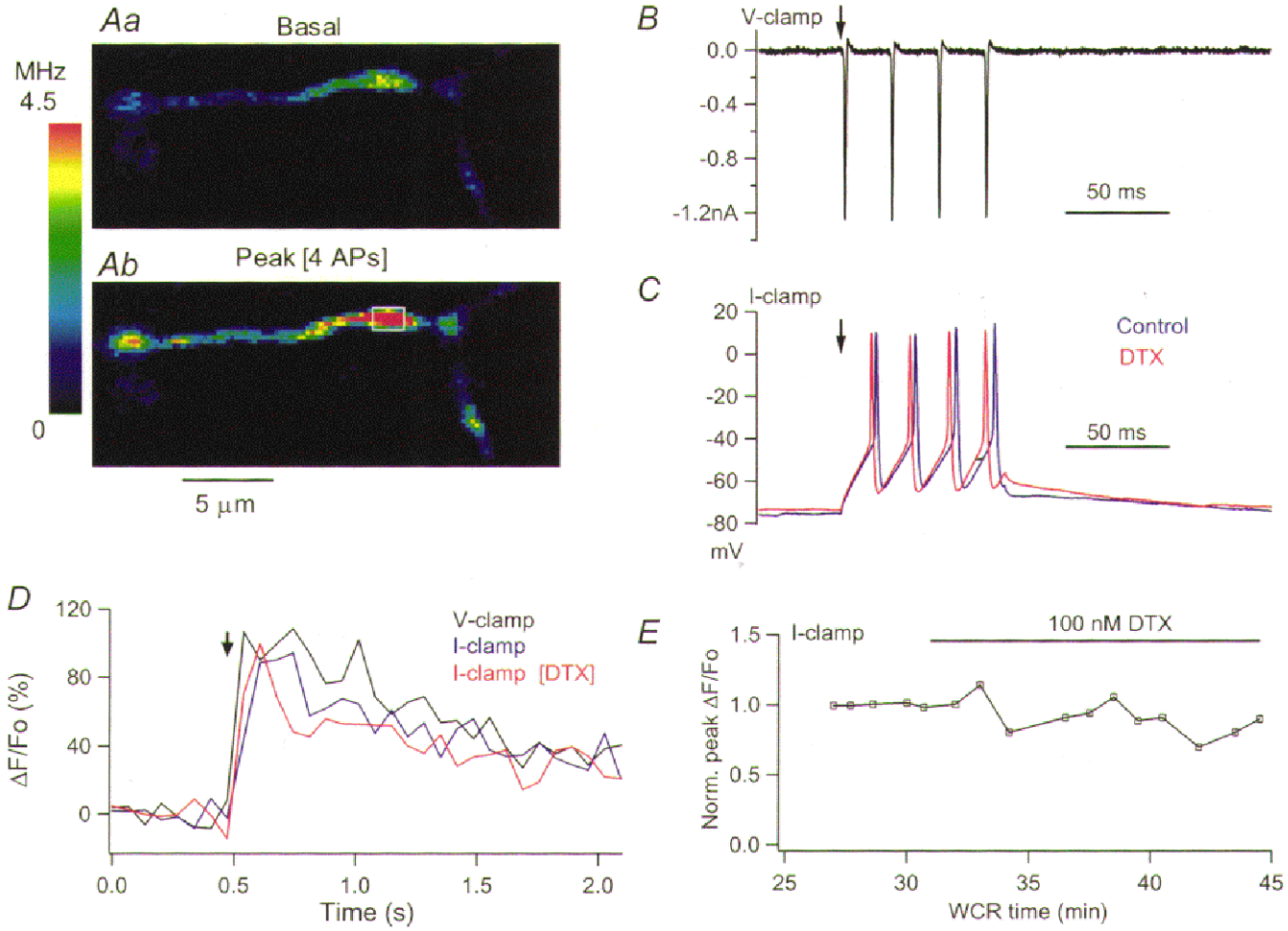

Figure 5. Lack of effect of αDTX on the action potential-evoked $[Ca^{2+}]_i$ rises in current-clamp recording

A, pseudocolour images obtained in control external saline at rest (*a*) and at the peak of the response to four action potentials elicited under current-clamp conditions by a 50 ms pulse of 65 pA (*b*). The blue traces in *C* and *D* display the corresponding membrane voltage and the time course of the $\Delta F/F_o$ for the ROI drawn in *Ab*. The black traces in *C* and *D* show, for the same experiment, the membrane currents and the $\Delta F/F_o$ transients evoked by four pulses of 3 ms duration applied under voltage-clamp conditions from a holding potential of −70 mV. The red traces in *C* and *D* show the action potentials and the time course of the $\Delta F/F_o$ transient for the same ROI, obtained under current-clamp conditions 7·5 min after addition of 100 nM αDTX. *E* shows the peak $\Delta F/F_o$ signals obtained under current-clamp conditions for the analysed ROI as a function of whole-cell recording time. The data were normalized to the average of the four responses in control saline. The stimulation parameters used to elicit the four action potentials under current-clamp conditions were the same throughout the recording (50 ms current pulse of 65 pA).

current-clamp conditions. Furthermore, the action potential waveforms in control and αDTX showed no significant differences (Fig. 5*C*). Similar results were obtained in four cells tested. Thus, αDTX does not alter somatic electrical signals or intracellular calcium transients at release sites, and this result stands independently of the stimulation protocol. Overall we conclude that under our recording conditions the αDTX-sensitive K^+ channels present in basket cell terminals do not contribute significantly to repolarization of the action potential.

We next tried the broad spectrum K^+ channel blocker 4-AP, which in expression systems blocks most of the subtypes of the Kv1, Kv2 and Kv3 channels tested so far (Table 1 in Mathie *et al.* 1998). 4-AP, at 5 mM, strongly reduced the K^+ currents recorded from basket cell terminals (Southan & Robertson, 1998*a*). As shown in Fig. 6, this blocker produced a clear increase in the peak amplitude of action potential-evoked $[Ca^{2+}]_i$ rises in basket cell axons. The upper panels display the images obtained at rest and at the peak of the $[Ca^{2+}]_i$ rise evoked by four action potentials, in control saline (*Aa* and *b*) and 3·5 min after addition of 0·25 mM 4-AP (*Ba* and *b*). The corresponding $\Delta F/F_o$ values as a function of time for two of the ROIs analysed in this axon are shown in Fig. 6*Ca* and *b* (open symbols correspond to control, closed symbols to 4-AP). Figure 6*D* shows the normalized peak $\Delta F/F_o$ for three ROIs, in all of which the action potential-evoked $[Ca^{2+}]_i$ rise was strongly augmented by 4-AP. In three cells tested, 0·25 mM 4-AP increased the peak $\Delta F/F_o$ induced by trains of four action potentials by 2·15. The increase was not significantly different (test/control, 2·26) in seven other cells where 4-AP was used at a concentration of 2·5 mM. These results were thus pooled in the summary presented in Fig. 8*A*. Similarly to the experiments described above for αDTX, and in accord with the findings of Southan & Robertson (1998*a*), 4-AP had no effect in the somatically recorded voltage-gated currents (data not shown).

CTX and TEA, both of which significantly increased the spontaneous release of GABA, differed both from αDTX and from 4-AP in their effects on intracellular calcium signalling as well as on the K^+ currents. In somatic recordings, CTX (100 nM) and TEA (2·5 mM) decreased by approximately 50% the depolarization-evoked K^+ currents (data not shown). At the same doses, neither of these blockers

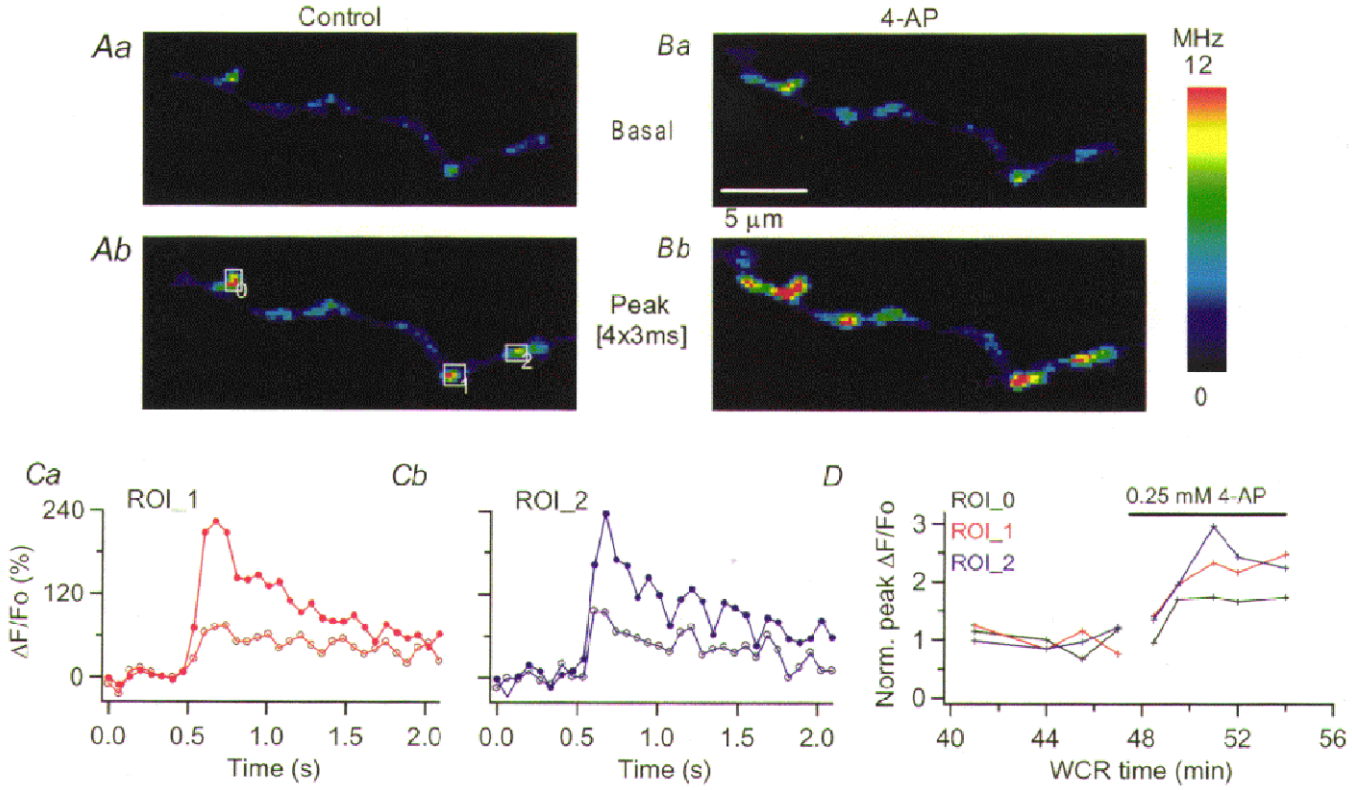

Figure 6. 4-AP enhances action potential-evoked $[Ca^{2+}]_i$ rises in basket cells axons

A, pseudocolour images obtained in control external saline at rest (*a*) and at the peak of the response to four action potentials (*b*). *Ba* and *b* show the corresponding images in the presence of 0·25 mM 4-AP. The position of the three ROIs analysed is given by the rectangles drawn in *Ab*. The time course of the $\Delta F/F_o$ signals evoked by four action potentials for two ROIs are shown in *Ca* and *b*. Open circles correspond to the signals under control conditions, filled circles to those at the peak of the 4-AP effect. *D* presents the normalized $\Delta F/F_o$ values as a function of whole-cell recording time for the three ROIs analysed.

affected the action potential-evoked intracellular calcium signals when used alone ($n = 5$ in both cases). However, if CTX or TEA were applied in conjunction with 4-AP (0·25 mM), the ensuing augmentation of the intracellular calcium signals was significantly larger than that caused by 4-AP alone. An example of these results is shown in Fig. 7, where panels in *A* present the time course of the $\Delta F/F_o$ changes induced in an axonal varicosity by one, four and eight action potentials in control saline (*a*), 6 min after addition of 100 nM CTX (*b*) and 9 min after exposure to CTX and 0·25 mM 4-AP (*c*). As with αDTX, CTX did not have any obvious effect on the $[Ca^{2+}]_i$ rises. However, if 4-AP was added while CTX was present, intracellular calcium signals were increased to such an extent that the amplitude of the $[Ca^{2+}]_i$ rises for one, four and eight action potentials were indistinguishable. Considering the parameters obtained from *in vitro* calibrations of OG1 (see Methods), it appears that in the presence of 4-AP + CTX saturation of the Ca^{2+} indicator was reached even for a single action potential. The normalized peak $\Delta F/F_o$ for four ROIs analysed in this cell are shown in Fig. 7*Ba–c*. Note that the ratio of peak $\Delta F/F_o$ for single action potentials in 4-AP + CTX over control reaches values above 10. Therefore, the pooled data shown in Fig. 8*A*, which were derived from intracellular calcium signals evoked by trains of four action potentials in order to allow comparisons with the experiments performed with the other blockers, underestimate the potency of the combined action of CTX or TEA plus 4-AP. The potentiation of the 4-AP effect was confirmed in six cells in the case of 4-AP + CTX and in four cells for 4-AP + TEA (reviewed in Fig. 8*A*). In both cases, Student's *t* test indicated that the groups differed significantly from the 4-AP group ($P < 0·01$ for the comparison of 4-AP + CTX *vs.* 4-AP; $P < 0·05$ for the comparison of TEA + 4-AP *vs.* 4-AP). No such interaction is expected between αDTX and 4-AP since the αDTX-sensitive channels are also blocked by 4-AP (reviewed by Mathie *et al.* 1998). Results were in line with this expectation (Fig. 8*A*).

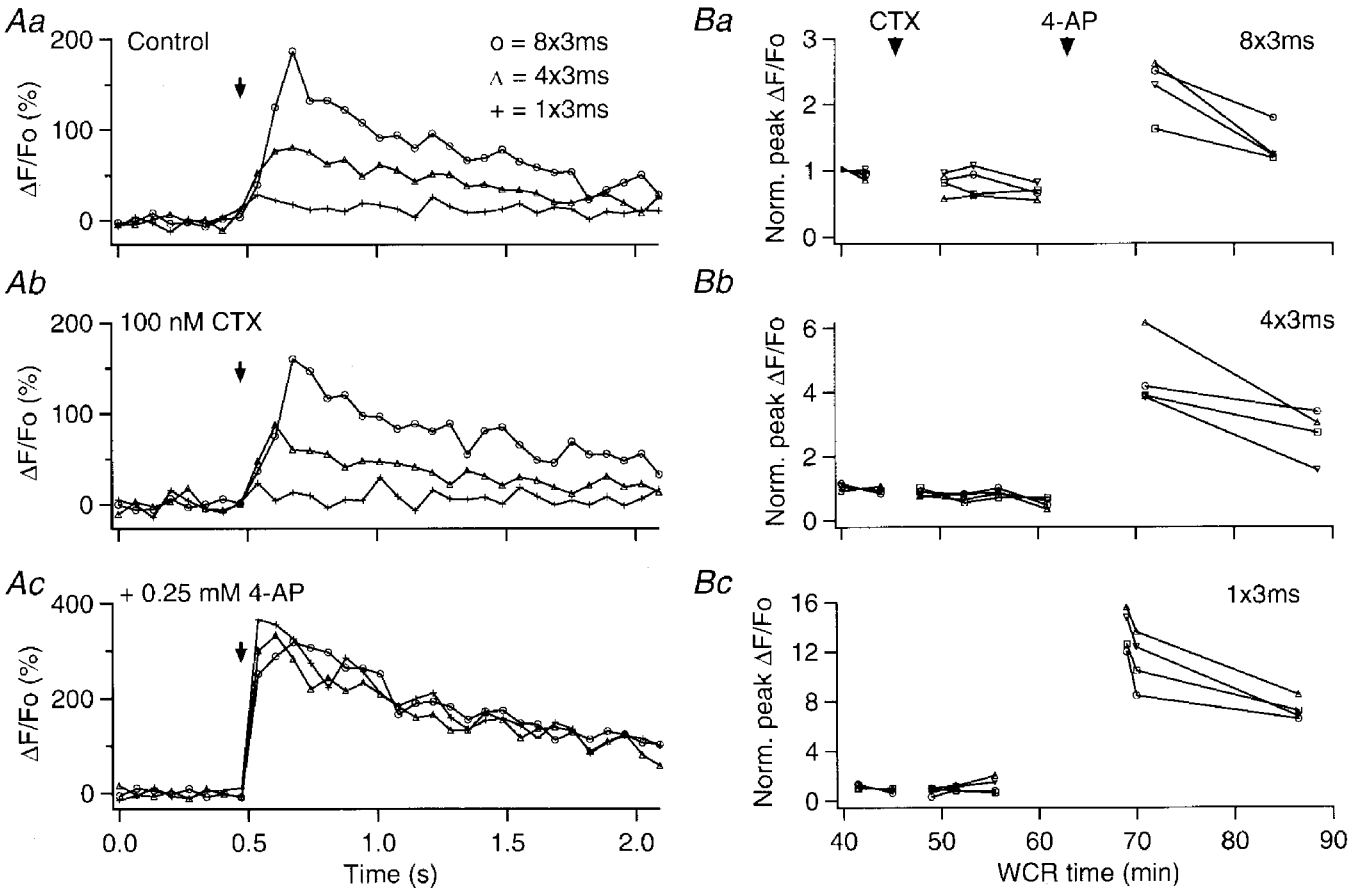

Figure 7. CTX does not affect action potential-evoked axonal $[Ca^{2+}]_i$ rises, but it enhances their augmentation by 4-AP

Aa, plot of the $\Delta F/F_o$ signals evoked by one (+), four (△) and eight (○) action potentials in an axonal ROI, while the slice was bathed in control saline. *Ab*, analysis of the same ROI in the presence of 100 nM CTX. *Ac*, corresponding plots after 0·25 mM 4-AP was added to the CTX-containing solution. The graphs in *B* show the peak $\Delta F/F_o$ signal values, normalized to the average of the two responses in control saline, for four ROIs analysed in the same axon, as a function of whole-cell recording time. *Ba*, normalized peak $\Delta F/F_o$ signals evoked by eight action potentials; *Bb*, normalized peak $\Delta F/F_o$ signals evoked by four action potentials; *Bc*, normalized peak $\Delta F/F_o$ signals evoked by one action potential.

The pharmacological analysis of action potential-evoked $[Ca^{2+}]_i$ rises in basket cells is summarized in Fig. 8*A*. Importantly, no distinction was found between the three types of axonal regions studied, namely terminals on Purkinje cell somata, branching points and varicosities, concerning the effects of any of the drugs tested. Therefore, results from the three types of structures have been pooled in Fig. 8*A*.

DISCUSSION

Two-photon intracellular calcium imaging of mammalian axons

Multiphoton excitation has numerous advantages over conventional non-confocal and confocal fluorescence imaging, and it has already yielded interesting information regarding dendritic intracellular calcium dynamics (reviewed by Denk & Svoboda, 1997; see references therein and Köster &

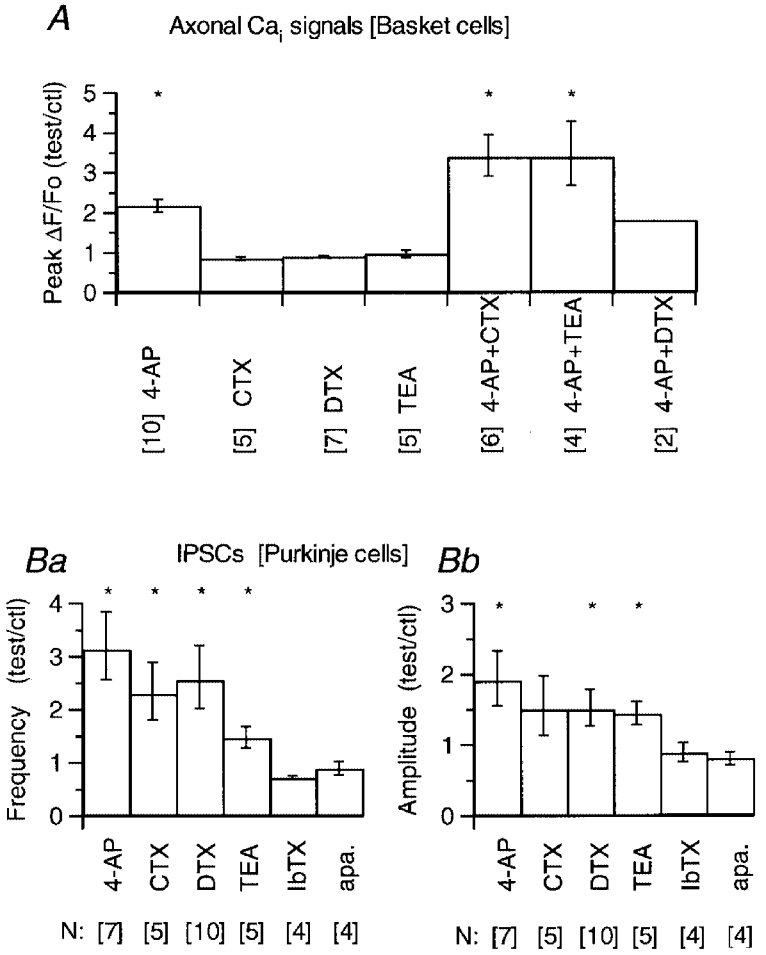

Figure 8. Summary of the effects of K^+ channel blockers on Purkinje cell IPSCs and in basket cell axonal $[Ca^{2+}]_i$ signals

A, basket cell axonal intracellular calcium (Ca_i) signals: all data included in this pool were obtained using trains of four action potentials. In each cell, three to six ROIs were analysed, and for each ROI the ratio of the peak $\Delta F/F_o$ value in the drug over that in control was calculated. When the effect of the drug faded with time (as in the experiment shown in Fig. 6 for the combined action of CTX and 4-AP) the value taken was that of the maximum. The ratios from all the ROIs for each cell were averaged, and these averages were pooled to yield the mean values given in each histogram. The 4-AP group includes three cells tested at 0·25 mM and 7 at 2·5 mM; the effects were not different at these concentrations (see text). αDTX and CTX were used at 100 nM, TEA at 2·5 mM. In the groups of CTX, TEA and αDTX plus 4-AP, the 4-AP concentration was 0·25 mM. The error bars represent S.E.M. *B*, IPSCs were recorded from Purkinje cells in the presence of 10 μM NBQX, 100 μM APV and, in some experiments, 1 μM bicuculline; no bicuculline was added in any of the experiments testing for effects of apamin (see Methods). Currents were acquired during 3–6 min in control saline and during a period of 6–10 min after the drug was added to the bathing solution. For each cell, the ratio of the mean frequency and mean amplitude in the drug over that in control was calculated. These ratios were averaged and are plotted in *Ba* and *b*. The error bars represent S.E.M. In *A* and *B* the numbers in brackets below the name of each drug correspond to the number of cells included in the pooled analysis. An asterisk on top of a bar denotes that the mean value was significantly different from 1 at the $P < 0·05$ level (Student's *t* test).

Sakmann, 1998 for a recent study on dendritic intracellular calcium signalling in cortical cells). We find the application of this technique to axonal intracellular calcium signalling particularly valuable. The inherent confocality of two-photon imaging greatly improves the spatial resolution, an important asset for accurate visualization of the small presynaptic terminals of mammalian axons. Furthermore, due to the highly restricted localization of the excitation, photodamage is significantly reduced compared with conventional imaging methods. This allowed us to record action potential-evoked $[Ca^{2+}]_i$ rises for the extended periods of time required to carry out pharmacological studies in brain slices.

Hierarchy of K^+ channels in basket cell axons

The present work suggests that two distinct classes of K^+ channels contribute to different degrees to the repolarization of presynaptic terminals in basket cell axons. 4-AP-sensitive, αDTX-insensitive K^+ channels have the major role, since their blockade significantly increases the action potential-evoked axonal $[Ca^{2+}]_i$ rises. K^+ channels sensitive to TEA and CTX have a secondary role: their blockade does not affect the magnitude of the $[Ca^{2+}]_i$ rises, indicating that repolarization can proceed normally in their absence. However, if the major channels are already blocked, these channels come into play to bring down membrane potential, albeit at a slower rate. This is supported by the finding that the increase in $[Ca^{2+}]_i$ rises was much augmented when 4-AP and CTX (or TEA) were applied jointly as compared to 4-AP alone. This hierarchy may arise from differences in channel density. Alternatively, distinct biophysical properties such as a lower voltage-activation threshold and/or a faster activation kinetics may render the 4-AP-sensitive, αDTX-insensitive K^+ channels better suited for fast repolarization of the synaptic terminals.

In agreement with the present results, 4-AP was found to be more effective than a number of other K^+ channel blockers, including αDTX, in increasing action potential duration at synapses between CA3 and CA1 hippocampal pyramidal cells (Wheeler *et al.* 1996). A related compound, 3,4 diaminopyridine, enhanced the action potential-evoked $[Ca^{2+}]_i$ rises measured at individual synaptic terminals in lizard motor nerves (David *et al.* 1997) and reduced considerably the voltage-gated K^+ currents recorded from synaptic varicosities at the *Xenopus* neuromuscular junction (Yazejian *et al.* 1997). On the other hand, a member of the Kv3 family (Kv3.1) has been proposed as the major K^+ channel at the calyx of Held (Forsythe, 1994). It is worth noting that immunocytochemical studies indicate that proteins of the Kv3 family are also present in cerebellar basket cells (Weiser *et al.* 1994; Laube *et al.* 1996). However, given the pharmacological profile of these channels, i.e. high sensitivity to TEA and 4-AP, and our finding on the potentiation by TEA of the 4-AP induced increase in intracellular calcium transients, it is unlikely that they contribute significantly to action potential-evoked $[Ca^{2+}]_i$ rises in basket cell axons.

Amongst the various subunits of voltage-gated K^+ channels described to date, several have a pharmacological profile similar to that of the channel primarily responsible for the repolarization of basket cell axons. These include voltage-gated K^+ channels formed by the Kv1.3, 1.4 and 1.5 α-subunits and those formed by Kv2.1 and 2.2 α-subunits. All of these subunits can co-assemble into channels which, in heterologous expression systems, have a low sensitivity to αDTX and to TEA but are blocked by 4-AP (Table I in Mathie *et al.* 1998; Table 4 in Coetzee *et al.* 1999). There are, to our knowledge, no immunocytochemical data on the cellular distribution of Kv1.5 channels in rat cerebellum; Kv1.4 channels have been reported to be absent from this brain region (Sheng *et al.* 1992). Kv1.3 channels, on the other hand, are found in basket cell axons (Veh *et al.* 1995) whereas Kv2.1 and 2.2 are present in the cerebellum (Table 4 in Coetzee *et al.* 1999). Therefore, channels formed by the Kv2 and/or the Kv1.3 α-subunits can be considered as good candidates for the control of the axonal action potential waveform in cerebellar basket cells. Unfortunately, without commercially available selective blockers, it is difficult to distinguish amongst these various proteins.

We have fewer clues for the possible molecular identity of the channels blocked by CTX and TEA. Both of these agents are known to act on Ca^{2+}-activated K^+ (BK) channels, whose presence in synaptic terminals has been demonstrated in several preparations (e.g. Yazejian *et al.* 1997). However, given that the enhancement of the spontaneous release of GABA caused by these blockers was not mimicked by Ibtx, a selective blocker of BK channels, it is unlikely that the effects we observed on axonal $[Ca^{2+}]_i$ rises are mediated by BK channels. In line with this interpretation, *in situ* hybridization studies using an antibody for the high conductance BK channel indicate that this channel is absent from the molecular layer of the cerebellum and particularly from basket cell terminals (Knaus *et al.* 1996). Therefore, CTX and TEA presumably exert their effect by acting on a voltage-gated channel, the identity of which remains to be determined.

Since functional αDTX-sensitive channels are clearly present in basket cell axons and since this toxin enhances the IPSCs at interneurone–Purkinje cell synapses (Southan & Robertson, 1998*a*,*b*; Figs 3*A*, 3*D* and 8*B* of the present work), it was surprising to find that αDTX had no effect on action potential mediated intracellular calcium signals. Thus, αDTX-sensitive channels, presumably having the Kv1.1 and/or Kv1.2 α-subunits, whose presence in basket cell axons has been ascertained immunocytochemically (McNamara *et al.* 1993, 1996; Sheng *et al.* 1994; Wang *et al.* 1994; Veh *et al.* 1995) alter neurotransmitter release through a mechanism distinct from that used by αDTX-insensitive, 4-AP-sensitive channels. As already discussed above, axonal K^+ channels may regulate neurotransmitter release by altering the spike threshold or the basal intracellular calcium concentration rather than the speed of action potential repolarization. The results obtained in terminal

recordings (Southan & Robertson, 1998*a*) suggest that, while 4-AP almost abolishes all voltage-dependent K^+ currents, αDTX blocks only one component of voltage-dependent K^+ channels that are primarily active in the voltage range close to the spike threshold (between −40 and −20 mV: Southan & Robertson, 1998*a*). In view of these results and of the present data it seems possible that the primary role of Kv1.1 and Kv1.2 channels could be to regulate the axonal resting membrane potential and/or the propagation of the action potential along the presynaptic axon.

Coetzee, W. A., Amarillo, A., Chiu, J., Chow, A., Lau, D., McCormack, T., Moreno, H., Nadal, M., Ozaita, A., Poutney, D., Saganich, M., Vega-Saenz de Miera, E. & Rudy, B. (1999). Molecular diversity of K^+ channel proteins. In *Molecular and Functional Diversity of Ion channels and receptors, Annals of the New York Academy of Sciences* **868** (in the Press).

David, G., Barrett, J. N. & Barrett, E. F. (1997). Stimulation-induced changes in $[Ca^{2+}]$ in lizard motor nerve terminals. *Journal of Physiology* **504**, 83–96.

Debanne, D., Guérineau, N. C., Gähwiler, B. H. & Thompson, S. M. (1997). Action-potential propagation gated by an axonal I_A-like K^+ conductance in hippocampus. *Nature* **389**, 286–289.

Denk, W. & Svoboda, K. (1997). Photon upmanship: why multiphoton imaging is more than a gimmick. *Neuron* **18**, 351–357.

DiGregorio, D. A. & Vergara, J. L. (1997). Localized detection of action potential-induced presynaptic calcium transients at a *Xenopus* neuromuscular junction. *Journal of Physiology* **505**, 585–592.

Eccles, J., Llinás, R. & Sasaki, K. (1966). The inhibitory interneurons within the cerebellar cortex. *Experimental Brain Research* **1**, 1–16.

Fierro, L. & Llano, I. (1996). High endogenous calcium buffering in Purkinje cells from rat cerebellar slices. *Journal of Physiology* **496**, 617–625.

Forsythe, I. D. (1994). Direct patch recordings from identified presynaptic terminals mediating glutamatergic EPSCs in the rat CNS, *in vitro*. *Journal of Physiology* **479**, 381–387.

Helmchen, F., Borst, J. G. J. & Sakmann, B. (1997). Calcium dynamics associated with a single action potential in a CNS presynaptic terminal. *Biophysical Journal* **72**, 1458–1471.

Hoffman, D. A., Magee, J. C., Colbert, C. M. & Johnston, D. (1997). K^+ channel regulation of signal propagation in dendrites of hippocampal pyramidal neurones. *Nature* **387**, 869–875.

Jackson, M. B., Konnerth, A. & Augustine, G. J. (1991). Action potential broadening and frequency-dependent facilitation of calcium signals in pituitary nerve terminals. *Proceedings of the National Academy of Sciences of the USA* **88**, 380–384.

Knaus, H.-G., Schwarzer, C., Koch, R. O. A., Eberhart, A., Kaczorowski, G. J., Glossmann, H., Wunder, F., Pongs, O. & Garcia, M. L. (1996). Distribution of high-conductance Ca^{2+}-activated K^+ channels in rat brain: targeting to axons and nerve terminals. *Journal of Neuroscience* **16**, 955–963.

Kosaka, T., Kosaka, K., Nakayama, T., Hunziker, W. & Heizmann, C. W. (1993). Axons and axon terminals of cerebellar Purkinje cells and basket cells have higher levels of parvalbumin immunoreactivity than somata and dendrites: quantitative analysis by immunogold labeling. *Experimental Brain Research* **93**, 483–491.

Köster, H. J. & Sakmann, B. (1998). Calcium dynamics in single spines during coincident pre- and postsynaptic activity depend on relative timing of back-propagating action potentials and subthreshold excitatory postsynaptic potentials. *Proceedings of the National Academy of Sciences of the USA* **95**, 9596–9601.

Laube, G., Röper, J., Pitt, J. C., Sewing, S., Kistner, U., Garner, C. C., Pongs, O. & Veh, R. W. (1996). Ultrastructural localization of *Shaker*-related potassium channel subunits and synapse-associated protein 90 to septate-like junctions in rat cerebellar pinceaux. *Molecular Brain Research* **42**, 51–61.

Llano, I., Marty, A., Armstrong, C. M. & Konnerth, A. (1991). Synaptic- and agonist-induced excitatory currents of Purkinje cells in rat cerebellar slices. *Journal of Physiology* **434**, 183–213.

Llano, I., Tan, Y. & Caputo, C. (1997). Spatial heterogeneity of intracellular Ca^{2+} signals in axons of basket cells from rat cerebellar slices. *Journal of Physiology* **502**, 509–519.

Lüscher, C., Lipp, P., Lüscher, H.-R. & Niggli, E. (1996). Control of action potential propagation by intracellular Ca^{2+} in cultured rat dorsal root ganglion cells. *Journal of Physiology* **490**, 319–324.

McNamara, N. M. C., Averill, S., Wilkin, G. P., Dolly, J. O. & Priestley, J. V. (1996). Ultrastructural localization of a voltage-gated K^+ channel α-subunit (Kv1.2) in the rat cerebellum. *European Journal of Neuroscience* **8**, 688–699.

McNamara, N. M. C., Muniz, Z. M., Wilkin, G. P. & Dolly, J. O. (1993). Prominent location of a K^+ channel containing the α-subunit Kv1.2 in the basket cell nerve terminals of rat cerebellum. *Neuroscience* **57**, 1039–1045.

Mathie, A., Woltorton, J. R. A. & Watkins, C. S. (1998). Voltage-activated potassium channels in mammalian neurones and their block by novel pharmacological agents. *General Pharmacology* **30**, 13–24.

Neher, E. (1995). The use of fura-2 for estimating Ca buffers and Ca fluxes. *Neuropharmacology* **34**, 1423–1442.

Neher, E., Llano, I., Hopt, A., Würriehausen, W. & Tan, Y. P. (1998). Fast scanning and efficient photodetection in a simple two photon microscope. *Biophysical Journal* **74**, A184.

Pouzat, C. & Marty, A. (1999). Somatic recording of GABAergic autoreceptor current in cerebellar stellate and basket cells. *Journal of Neuroscience* **19**, 1675–1690.

Ramón y Cajal, S. (1911). *Histologie du système nerveux de l'homme et des vertebrés*. Maloine, Paris.

Regehr, W. G. & Atluri, P. P. (1995). Calcium transients in cerebellar granule cells presynaptic terminals. *Biophysical Journal* **68**, 2156–2170.

Röper, J. & Pongs, O. (1996). Presynaptic potassium channels. *Current Opinion in Neurobiology* **6**, 338–341.

Seutin, V., Scuvee-Moreau, J. & Dresse, A. (1997). Evidence for a non-GABAergic action of quaternary salts of bicuculline on dopaminergic neurones. *Neuropharmacology* **36**, 1653–1657.

Sheng, M., Tsaur, M.-L., Jan, Y. N. & Jan, L. Y. (1992). Subcellular segregation of two A-type K^+ channel proteins in rat central neurons. *Neuron* **9**, 271–284.

Sheng, M., Tsaur, M.-L., Jan, Y. N. & Jan, L. Y. (1994). Contrasting subcellular localization of the mKv1.2 K^+ channel subunit in different neurons of the rat brain. *Journal of Neuroscience* **14**, 2408–2417.

Sinha, S. R., Wu, L.-G. & Saggau, P. (1997). Presynaptic calcium dynamics and transmitter release evoked by single action potentials at mammalian central synapses. *Biophysical Journal* **72**, 637–651.

Southan, A. P. & Robertson, B. (1998*a*). Patch-clamp recordings from cerebellar basket cell bodies and their presynaptic terminals reveal an asymmetric distribution of voltage-gated potassium channels. *Journal of Neuroscience* **18**, 948–955.

Southan, A. P. & Robertson, B. (1998*b*). Modulation of inhibitory post-synaptic currents (IPSCs) in mouse cerebellar Purkinje and basket cells by snake and scorpion toxin K^+ channel blockers. *British Journal of Pharmacology* **125**, 1375–1381.

Stuart, G., Spruston, N., Sakmann, B. & Häusser, M. (1997). Action potential initiation and backpropagation in neurons of the mammalian CNS. *Trends in Neurosciences* **20**, 125–131.

Stühmer, W., Ruppersberg, J. P., Schröter, K. H., Sakmann, B., Stocker, M., Giese, K. P., Perschke, A., Baumann, A. & Pongs, O. (1989). Molecular basis of functional diversity of voltage-gated potassium channels in mammalian brain. *EMBO Journal* **8**, 3235–3244.

Tan, Y. P., Llano, I., Hopt, A., Würriehausen, F. & Neher, E. (1999). Fast scanning and efficient photodetection in a simple two photon microscope. *Journal of Neuroscience Methods* (in the Press).

Veh, R. W., Lichtinghagen, R., Sewing, S., Wunder, F., Grumbach, I. M. & Pongs, O. (1995). Immunohistochemical localization of five members of the K_v1 channel subunits: contrasting subcellular locations and neurone-specific co-localization in rat brain. *European Journal of Neuroscience* **7**, 2189–2205.

Vincent, P. & Marty, A. (1996). Fluctuations of inhibitory postsynaptic currents in Purkinje cells from rat cerebellar slices. *Journal of Physiology* **494**, 183–199.

Wang, H., Kunkel, D. D., Martin, T. M., Schwartzkroin, P. A. & Tempel, B. L. (1993). Heteromultimeric K^+ channels in terminal and juxtaparanodal regions of neurones. *Nature* **365**, 75–79.

Wang, H., Kunkel, D. D., Schwartzkroin, P. A. & Tempel, B. L. (1994). Localization of Kv1.1 and Kv1.2, two K channel proteins, to synaptic terminals, somata and dendrites in the mouse brain. *Journal of Neuroscience* **14**, 4588–4599.

Weiser, M., Vega-Saenz de Miera, E., Kentros, C., Moreno, H., Franzen, L., Hillman, D., Baker, H. & Rudy, B. (1994). Differential expression of Shaw-related K^+ channels in the rat central nervous system. *Journal of Neuroscience* **14**, 949–972.

Wheeler, D. B., Randall, A. & Tsien, R. W. (1996). Changes in action potential duration alter reliance of excitatory synaptic transmission on multiple types of Ca^{2+} channels in rat hippocampus. *Journal of Neuroscience* **16**, 2226–2237.

Wu, L.-G. & Saggau, P. (1997). Presynaptic inhibition of elicited neurotransmitter release. *Trends in Neurosciences* **20**, 204–212.

Xia, Z. & Storm, D. R. (1997). Calmodulin-regulated adenylyl cyclases and neuromodulation. *Current Opinion in Neurobiology* **7**, 291–296.

Yazejian, B., DiGregorio, D. A., Vergara, J. L., Poage, R. E., Meriney, S. D. & Grinnell, A. D. (1997). Direct measurements of presynaptic calcium and calcium-activated potassium currents regulating neurotransmitter release at cultured *Xenopus* nerve-muscle synapses. *Journal of Neuroscience* **17**, 2990–3001.

Zhang, C.-L., Messing, A. & Chiu, S. Y. (1999). Specific alteration of spontaneous GABAergic inhibition in cerebellar Purkinje cells in mice lacking the potassium channels Kv1.1. *Journal of Neuroscience* **15**, 2852–2864.

Acknowledgements

The two-photon scanning microscope used in the present work was developed in collaboration with E. Neher, whom we thank for giving us the opportunity of working with him on this stimulating project. We thank A. Marty for his support and lively discussions throughout this work and for his comments on the manuscript, C. Pouzat for sharing with us his unpublished data on Purkinje cell IPSCs and B. Rudy for helpful discussions. We thank R. Bookman for providing the Pulse Control software.

Corresponding author

I. Llano: Arbeitsgruppe Zelluläre Neurobiologie, Max-Planck-Institut für biophysikalische Chemie, Am Fassberg, D-37070 Göttingen, Germany.

Email: illano@gwdg.de

Author's permanent address

Y. P. Tan: Boğaziçi University, BMME, PK 2 Istanbul, Turkey.